Flow Simulation in a Submerged Membrane Bioreactor at Laboratory Scale

Y.M. Carreño-Martinez*, J.M. Gozálvez-Zafrilla, J.A. Mendoza-Roca, A. Santafé-Moros
Institute for Industrial, Radiological and Environmental Safety (ISIRYM), Universidad Politécnica de Valencia, Spain
*Universidad Politécnica de Valencia (Dpto. Ing. Química y Nuclear). C/ Camino de Vera s/n. 46022 Valencia (Spain). E-mail: yencarma@posgrado.upv.es

Abstract: Submerged membrane bioreactor (SMBR) is an efficient technology for wastewater treatment that combines biological process and membrane filtration in one single stage. In the most usual configuration, submerged membrane hollow fibers are set in several panels. Air is introduced from the bottom in order to supply oxygen to the microorganisms but also to reduce fouling over the membrane fibers. The shear stress over the membrane surface is the main variable that contributes to fouling minimization. In this work, we have modeled a laboratory set-up to study how air injection contributes to have the suitable hydrodynamic conditions for fouling minimization. In this case we have used water as reference fluid as a first approach. Using the Bubbly flow and Convection & diffusion modes, the effects of bubble size and air flow were studied. An image analysis technique was used to measure the experimental bubble size distribution in the two-phase system.

Keywords: Bubbly flow, membrane bioreactor, fouling

1. Introduction

Combining membrane technology with biological reactor for the treatment of wastewater has led to development of the membrane bioreactors. Membrane bioreactor (MBR) is a variation of the conventional activated sludge treatment where the secondary settler is replaced by a membrane process (ultrafiltration or microfiltration) for the separation of the treated effluent from the sludge [1]. This system has been widely used due to their advantages over the conventional process. Their main advantages are the control of the solid concentration, a high effluent quality, good retention of all microorganisms and viruses, maintenance of high biomass concentration, and a real compactness [2].

Thus, in regions with water scarcity, the MBR process has a promising future since wastewater reuse is a necessity and the quality of its effluent is higher than that obtained by a conventional activated sludge system.

Two main MBR designs exist with the membrane module either located externally to the bioreactor (side stream) or immersed directly into it (SMBR). SMBR are preferred for large-scale use such as municipal wastewater treatment [3]. In this configuration coarse aeration is provided to the system not only to provide oxygen to the biomass, but also to limit particle deposition at the membrane surface (membrane fouling) by means of the shear stress generated. However, the membrane fouling is a major obstacle to the wide application of SMBRs, because it reduces permeability and increases investment and operating costs. For this reason, efforts to optimize the process are focused mainly on the development of models to describe the mass transfer mechanisms and dynamic behavior of the phenomena of membrane fouling, as well as new techniques for fouling control and minimization [4].

The membrane characteristics, biomass properties and the hydrodynamic conditions are parameters that affect at membrane fouling phenomena. The most effective strategy for fouling control is related to the velocity of the air bubbles introduced into the system. The shear stress generated near to the membrane surface by the bubble rise velocity, causes a physically movement of the concentration polarization layer and removes the material deposited on the membrane. Therefore, the fouling rate in an SMBR is a function mainly of the aeration intensity, the size porous of the diffuser, and configuration and the submerged membrane module.

Wicaksana et al [5] concluded that bubbles play multiple roles in controlling fouling, including inducing shear on the membrane surface as well as promoting fiber movement. As

well, they suggested that there is a potential benefit from smaller, rather than larger bubbles.

In addition to computational fluid dynamics has been used to assess mixing regime for pilot and full scale MBR plants [6,7].

This work is a first approach to investigate the influence of bubble size and gas flow rate on the hydrodynamic conditions that contribute to minimize fouling on the membrane surface. An experimental set-up was used to characterize the bubbly flow in water and to obtain results for the further COMSOL modeling.

2. Experimental

The SMBR laboratory set-up with a hollow fiber membrane module made of polyvinylidene fluoride (Nitto Denko Co.) was used to determine the distribution bubble size. Figure 1 shows a diagram of the laboratory set-up and Figure 2 shows a picture of the system in operation. Water was used as a reference fluid at a temperature of 298 K.

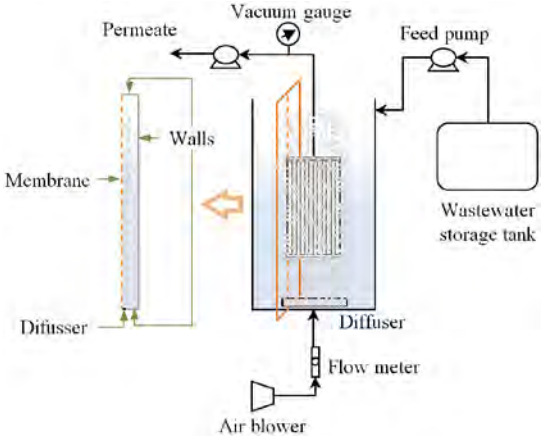

Figure 1. Laboratory set-up used in the experiments.

Figure 2. Image of the bubbly flow in the system.

2. Bubble size distribution

A high-speed photo camera was used to characterize the bubbly diameter distribution. High resolution images were taken of the flow established in the experimental set-up during operation. Then, an image analysis technique was applied to obtain the dimensions and volume of the individual bubbles. The equivalent diameter was calculated using the volume of the bubbles (1).

$$d = \sqrt{\frac{6 \cdot V_b}{\pi}} \qquad (1)$$

The equivalent diameter data were statistically analyzed using the distribution fitting tool of Matlab®. Figure 3 shows the histogram and the fitted distribution. Of the different probability distributions, the log-normal distribution obtained the better fit. Additionally, this distribution has the advantage of not including negative diameter values.

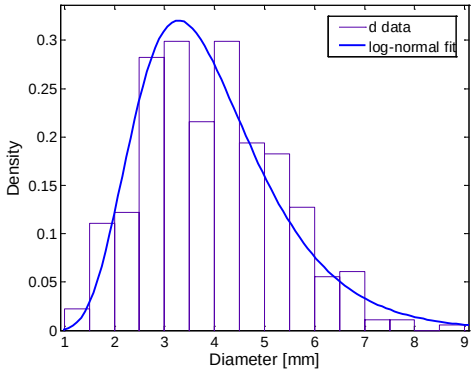

Figure 3. Bubbly diameter data and fitted log-normal distribution.

Table 1 shows the statistical properties and parameters of the fitted distribution. The parameters were used to calculate, using the cumulative form of the distribution, the diameters d_{10} and d_{90} (also shown in Table 1) that are the diameters for which 10% and 90% of the bubbles are respectively smaller. The mean value of the diameter was used as a representative value for the gas phase definition of the domain. We also performed calculations using the diameters d_{10} and d_{90}. In this way, a

confidence band between the curves for d_{10} and d_{90} was obtained. It is expected that the behavior of the real distributed bubbly flow be comprised in this region.

Table 1: Statistical properties and parameters of the log-normal distribution

Parameter		Value
Log-normal parameters	μ_d	1.315 mm
	σ_d	0.356 mm
Statistics	Mean	3.97 mm
	Variance	2.12 mm^2
Diameters	d_{10} (10%)	2.36 mm
	d_{90} (90%)	5.88 mm

3. Modeling

3.1 Domain geometry

The domain geometry was simplified to a 2D geometry as shown in Figure 4. First, it was considered that as dimension 'a' is significantly greater than dimension 'b', the problem can be solved as a two-dimensional one. Second, it was taken into account that the membrane array divides the set-up into two chambers with symmetrical flow with half of the entering gas flow *Q*.

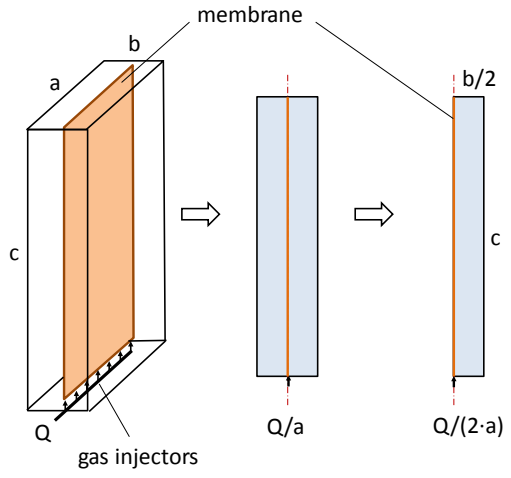

Figure 4. Simplification of the domain geometry.

In the experimental set-up, the gas inlets have pore size and are aligned in the tube place under the membrane. In the geometry, a dimension 'e' was assigned to this boundary (Figure 5). For e/b < 1/20, no significant difference was observed in the calculation results. Therefore, we arbitrarily assigned this dimension to the average bubble diameter determined in section 2.

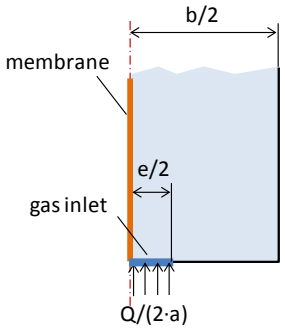

Figure 5. Detail of gas inlet.

3.2 Physics and domain settings

To obtain the model of the system, we used the "Bubbly Flow k-ε, turbulent model" of the Chemical Engineering Toolbox of COMSOL Multiphysics.

This mode is a particular case of two-phase flow.

Physics:

It was required the liquid and gas properties and the magnitude of the gravity component (Table 2).

Table 2: Domain properties and settings

Variable	Value
Temperature	T = 298 K
Water density	ρ_l = 997.1 kg/m^3
Water viscosity	μ_l = 8.903×10^{-4} Pa·s
Average molecular mass of air	M = 28.84 g/mol
Gravity (y-component)	g = -9.806 m/s^2

Slip model:

We used a pressure/drag balance model for large bubbles [8] as more than 90% of the bubbles were greater than 2 mm. As discussed in section 2, calculations were independently performed for the average bubble diameter d_m = 3.97 mm, but also for the selected limits d_{10} = 2.36 mm and d_{90} = 5.88 mm.

For this model, the surface tension coefficient at 298 K was also needed (71.99 dyne/m) [9].

Mass transfer:

No mass transfer model was considered as the dissolution of gas in water was neglected.

3.4 Boundary conditions

Figure 6 shows the fluid domain limited by the boundaries and the location of the point condition P1.

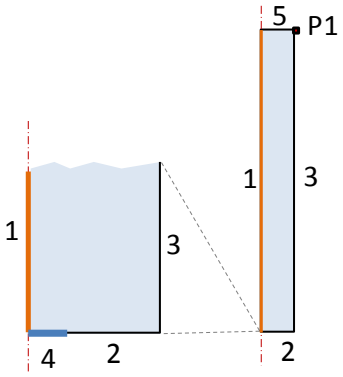

Figure 6. Boundaries of the domain.

Liquid phase:

Table 3 shows the boundary conditions for the liquid phase. Additionally a point constraint was set at the right upper corner (Pressure = 0).

Table 3: Boundary conditions for Bubbly Flow model (Liquid phase)

Boundary	Type	Value
1, 2, 3, 4	Logarithmic wall	wall offset
5	Slip	

Gas phase:

Table 4 shows the boundary conditions for the gas phase. The gas mass flux ($kg \cdot m^{-2} \cdot s^{-1}$) was calculated from the total gas flow. The calculations were performed for three values of volumetric gas flow (Q = 1, 2 and 4 L/min)

Table 4: Boundary conditions for Bubbly Flow model (Gas phase)

Boundary	Type	Value
1, 2, 3	Insulation	
4	Gas mass flux	Q/(2·a·e)
5	Gas outlet	

3.5 Meshing

The mesh used had 2400 triangular elements with 26218 degrees of freedom. The presence of boundary 4 force a more refined mess

3.6 Solver

To facilitate convergence, the problem was firstly solved for the smallest bubble size in transient state. Then, the final step was used as an initialization for the steady-state calculation. Then, the parametric solver was used to solve for the two remaining bubble sizes.

A direct solver (UMFPACK) was suitable to solve the problem as the number of d.o.f. was not high.

4. Results

The calculations yield to the knowledge of gas and liquid velocities, slip velocity and volume fraction of gas in the whole domain. The slip velocity is the relative velocity between the bubbles and the liquid.

In the example of Figure 7, it can be seen how the rise of the gas flow induces a rotational liquid movement.

For our study, the relevant information is the fluid conditions on the membrane surface. The bubble rise induces a shear rate on the membrane surface that contributes to minimize membrane fouling. Equation (2) relates the shear rate γ with

the superficial gas velocity U_g through a consistence index K and a flow behavior index n (n = 1 for Newtonian fluid) [10]. Considering this equation, a high superficial gas velocity is desirable to minimize membrane fouling.

$$\gamma = \left(\frac{\rho_l g U_g}{K} \right)^{1/n+1} \quad (2)$$

Figure 8 shows the liquid velocity profiles obtained for three entering gas flows. The results were similar for the three bubble diameters considered. On the contrary, Figure 9 shows the gas velocity profiles, which are influenced by the diameter. For bubbles with diameter smaller than 2 mm, the experimental results show that the gas rising velocity increases with the bubble size. On the contrary, for bubbles between 2 mm and approximately 5.5 mm, the greater the diameter, the smaller the slip velocity [11] what agrees with the calculation results.

The liquid velocities observed are very low to prevent fouling; besides the highest values are only obtained near the membrane bottom. However, gas velocity is enough to induce local shear effects and it has significant values along the entire membrane surface.

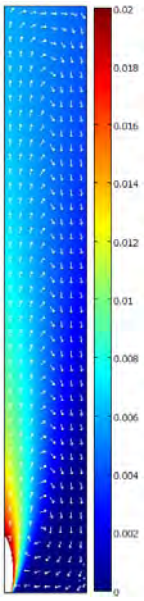

Figure 7. Volume fraction of gas and liquid velocity field (gas flow = 2 L/min, bubble diameter = 3.97 mm).

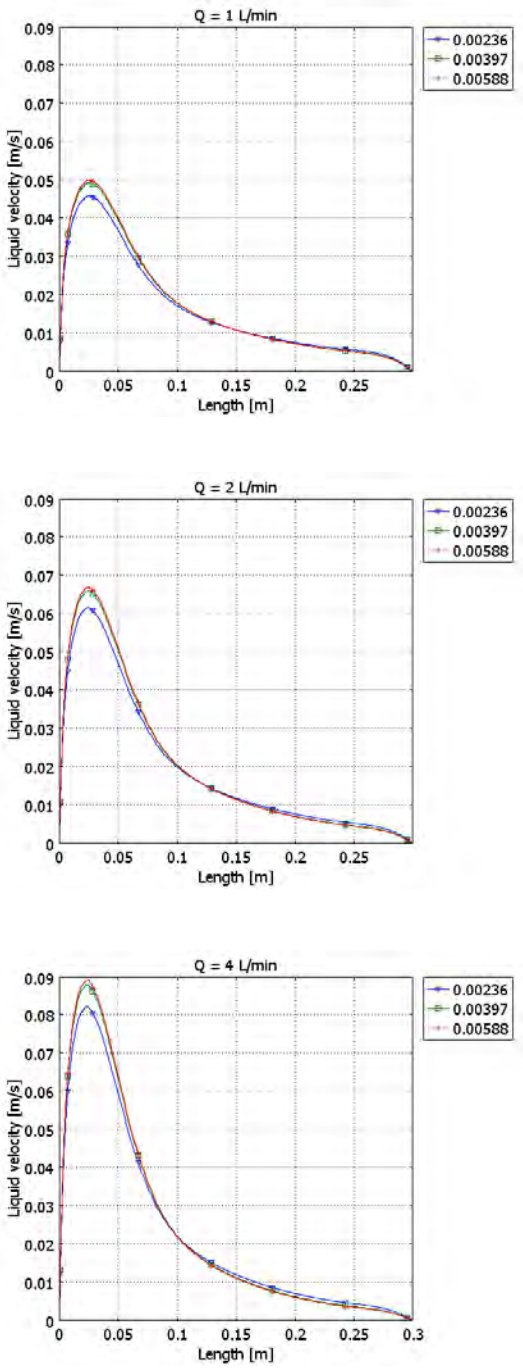

Figure 8. Liquid velocity at the boundary layer for three bubble sizes (Gas flow, Q = 1, 2, 4 L/min)

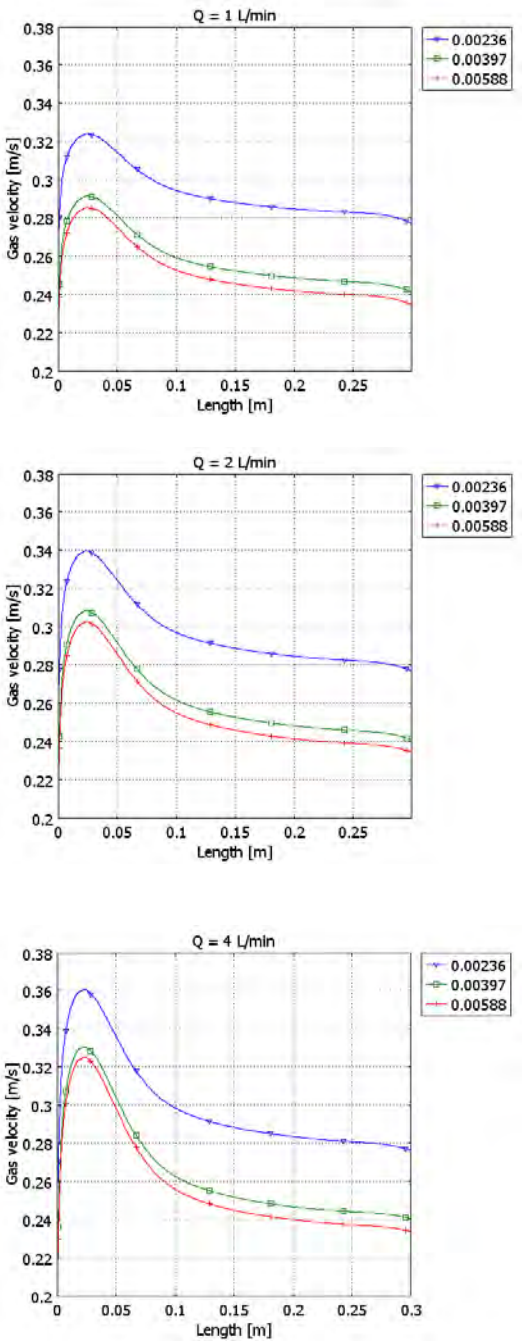

Figure 9. Gas velocity at the boundary layer for three bubble sizes (Gas flow, Q = 1, 2, 4 L/min)

Therefore, in order to minimize fouling, a modification of the gas injectors should be desirable in order to obtain most of the bubbles with diameters near to 2 mm. This would also have the beneficial effect of increasing the oxygen transfer which is important in a SMBR system.

The results also show that the volume fraction of gas was not influenced by the bubble size. Therefore, the value of the gas fraction can only be increased either by a higher gas flow (Figure 10) or by future modifications of the system geometry.

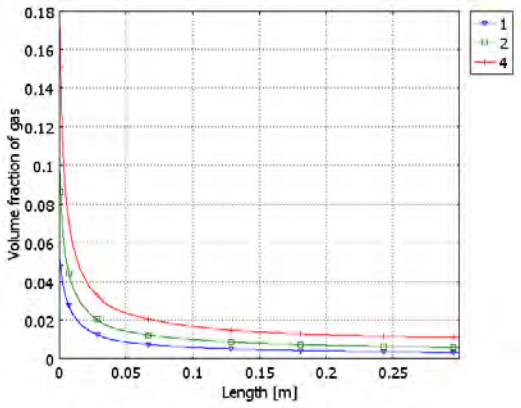

Figure 10. Volume fraction of gas at the boundary layer for Q = 1, 2 and 4 L/min.

5. Conclusions

COMSOL Multiphysics was used to obtain an initial model for the bubbly flow in an experimental set-up of an SMBR. In particular, the gas velocity near to the membrane surface is interesting to evaluate the shear rate effects on the membrane surface. The results obtained are useful for future modifications intended to minimize membrane fouling.

6. References

1. T. Stephenson, S. Judd, B. Jefferson, K. Brindle, Membrane bioreactors for wastewater treatment, *IWA-publishing*, London, 3-7 (2000).
2. M.E. Hernández Rojas, R. Van Kaam, S. Schetrite and C. Albasi, Role and variations of supernatant compounds in submerged membrane bioreactor fouling, *Desalination*, **179**, 95–107 (2005).
3. P. Le-Clech, B. Jefferson, S.J. Judd, A comparison of submerged and sidestream tubular membrane bioreactor configurations, *Desalination*, **173**, 113-122 (2005).
4. F. Meng, S.R. Chae, A. Drews, M. Kraume, H.S. Shin, F. Yang, Recent advances in membrane bioreactors (MBRs): Membrane fouling and membrane material, *Water Research*, **43**, 1489 – 1512 (2009).
5. F. Wicaksana, A. G. Fane, V. Chen, Fibre movement induced by bubbling using submerged hollow fibre membranes, *Journal of Membrane Science*, **271**, 186–195 (2006).
6. M.W.D. Brannock, H. De Wever, Y. Wanga, G. Leslie, Computational fluid dynamics simulations of MBRs: Inside submerged versus outside submerged membranes, *Desalination*, **236**, 244–251 (2009).
7. M. Brannock, Y. Wang, G. Leslie, Mixing Characterisation of Full-Scale Membrane Bioreactors: CFD Modelling with Experimental Validation, *Water Research*, **44**, 3181-3191 (2010).
8. A. Sokolichin, G. Eigenberger, and A. Lapin, Simulations of Buoyancy Driven Bubbly Flow: Established Simplifications and Open Questions, *AIChE Journal*, **50**, 24–49 (2004)
9. E.W. Lemmon et al., "Thermophysical Properties of Fluid Systems" en NIST Chemistry WebBook, NIST Standard Reference Database http://webbook.nist.gov (obtained 2010/09).
10. J.A. Sánchez-Pérez, E.M. Rodríguez-Porcel, J.L. Casas López, J.M. Fernández Sevilla, Y. Chisti, Shear rate in stirred tank and bubble column bioreactors, *Chemical Engineering Journal*, **124,** 1–5 (2006)
11. M. A. R. Talaia, Terminal velocity of a bubble rise in a liquid column, *World Academy of Science, Engineering and Technology*, **28**, 264-268 (2007)

7. Acknowledgements

The Universidad Politécnica de Valencia is kindly acknowledged for the project PAID-06-08-3287.

8. List of symbols

d bubble effective diameter, mm
g gravity, $m \cdot s^{-2}$
K consistence index
n flow behavior index
Q gas flow input, $L \cdot min^{-1}$
U_g average superficial gas velocity, $m \cdot s^{-1}$
V_b bubble volume, mm^3

γ shear rate, s^{-1}
μ_l liquid viscosity, $Pa \cdot s^{-1}$
ρ_l liquid density, $m \cdot s^{-1}$